ISBN: 978-3-95450-184-7 doi:10.18429/JACoW-IPAC2018-TUPML041

TWO-STAGE LASER-DRIVEN PLASMA ACCELERATION WITH EXTERNAL INJECTION FOR EuPRAXIA*

E. N. Svystun†, R. W. Assmann, U. Dorda, A. Ferran Pousa[1], T. Heinemann[1], B. Marchetti, A. Martinez de la Ossa[1], P. A. Walker, M. K. Weikum, J. Zhu, Deutsches Elektronen-Synchrotron, DESY, 22607 Hamburg, Germany
[1]also at University of Hamburg, 20148 Hamburg, Germany

Abstract

The EuPRAXIA (European Particle Research Accelerator with eXcellence In Applications) project aims at producing a conceptual design for the worldwide plasma-based accelerator facility, capable of delivering multi-GeV electron beams with high quality. This accelerator facility will be used for various user applications such as compact X-ray sources for medical imaging and high-energy physics detector tests. EuPRAXIA explores different approaches to plasma acceleration techniques. Laser-driven plasma wakefield acceleration with external injection of an RF-generated electron beam is one of the basic research directions of EuPRAXIA. We present studies of electron beam acceleration to GeV energies by a two-stage laser wakefield acceleration with external injection from an RF accelerator. Electron beam injection, acceleration and extraction from the plasma, using particle-in-cell simulations, are investigated.

INTRODUCTION

The remarkable progress in laser technology over the past decade [1, 2] allows Laser-plasma accelerators (LPA) to be seen as the leading technology in advanced accelerators standing out through enormous accelerating gradients on the order of 10-100 GV/m [3]. However, despite prominent experimental and theoretical achievements in the field of laser wakefield acceleration (LWFA), among others the demonstration of the production of GeV-class electron beams [4, 5], the realization of a LPA matching the demanding requirements on beam quality and stability for applications such as Free-Electron-Lasers (FEL) remains a challenge. Key parameters of electron beams delivered by LPAs, such as energy spread and normalized emittance, are still worse than those achieved in conventional accelerators. Limitations on the quality of laser-plasma-accelerated electron beams may arise from laser instabilities, plasma density fluctuations, scarce control over the beam injection process, etc.

There are different mechanisms of producing electron beams for acceleration in a plasma in LPAs. The electron beam can be produced internally by trapping the plasma background electrons, or it can be prepared externally, e.g. by an RF gun, etc. The external injection of an electron beam from a conventional electron linac into a plasma is a promising method for the production of FEL-capable beams in plasma-based accelerators (PBAs) due to the sufficient control over the initial parameters of an electron beam injected into an acceleration stage. Well-established technologies of conventional accelerators allow electron beams of high quality (small transverse emittance and energy spread), high stability and reproducibility (control of accelerated charge, tuning beam energy, etc.) to be delivered.

In this paper, we present an extension of numerical studies reported in [6] on quality-preserving acceleration of an electron beam by a laser-driven plasma accelerator with external injection from an RF linac. These studies have been carried out in the context of EuPRAXIA [7]. The Horizon 2020 project EuPRAXIA is preparing a conceptual design report of a highly compact and cost-effective plasma-based European facility with multi-GeV electron beams.

RESULTS AND DISCUSSION

Previous studies [6] for the first set of EuPRAXIA laser pulse parameters and a plasma density of $n_0 = 10^{17}$ cm^{-3} showed that the laser pulse defocusing starts to play a considerable role at distances of the order of 2-3 cm, thus limiting the length of the acceleration region. Another factor that limits the acceleration process in LPAs is laser diffraction, the characteristic distance of which is the Rayleigh length:

$$z_R = \frac{w_0^2 \pi}{\lambda_l},$$

where w_0 is the laser spot size at the focus and λ_l is the laser wavelength.

In the studies presented in this paper, the laser pulse defocusing and diffraction were counteracted by transverse plasma density tailoring, that allowed the laser pulse to be guided. This in turn enabled the acceleration region to be extended to lengths greater than the Rayleigh length, and the laser pulse energy and power to be reduced.

A two-dimensional simulation has been carried out with the particle-in-cell (PIC) code OSIRIS [8]. The following laser pulse parameters were assumed: pulse length $\tau_l = 70$ fs (FWHM); spot size $w_0 = 50$ µm; normalized peak intensity $a_0 = 2.7$; wavelength $\lambda_l = 800$ nm; peak power $P_L \approx 612$ TW. The laser transverse and temporal profiles are Gaussian. The laser pulse and the electron beam are injected collinearly into a plasma channel with a

* Work supported by the European Unions Horizon 2020 research and innovation programme under grant agreement № 653782.
† email address: elena.svystun@desy.de

ISBN: 978-3-95450-184-7 doi:10.18429/JACoW-IPAC2018-TUPML041

Table 1: Electron Beam Parameters at the Plasma Entrance

Charge, Q [pC]	5.6
Mean energy, $\bar{E}$ [MeV]	101
Relative energy spread, $\Delta E/\bar{E}$ [%]	0.43
Longitudinal RMS size, $\sigma_{z;rms}$ [μm]	0.59
Transverse RMS size, $\sigma_{x;rms}$ [μm]	2.55
Beta-function, β_x [mm]	2.76
Normalized transverse emittance, $\epsilon_{n;x}$ [μm]	0.47

radially parabolic density profile of the form $n(r) = n_0 + \Delta n(r/r_{ch})^2$, where the channel depth $\Delta n = 0.452 n_0$, the channel width $r_{ch} = 50$ μm and the on-axis plasma density $n_0 = 10^{17}$ cm^{-3}. The plasma wavelength is $\lambda_p = 106$ μm and the plasma skin depth is $c/\omega_p = k_p^{-1} = 16.8$ μm, with the plasma frequency given by $\omega_p = (n_0 e^2/\varepsilon_0 m_e)^{1/2}$, where c is the speed of light, k_p is the plasma wave number, e is the electron charge, ε_0 is the vacuum permittivity and m_e is the electron mass. The temporal offset between the electron beam center and the laser pulse center is equal to 294 fs (88.22 μm).

The simulation was conducted by employing a speed-of-light moving window with the longitudinal and transverse sizes of $(11 \times 20)\, k_p^{-1}$ and a resolution of $(0.00095 \times 0.0588)\, k_p^{-1}$. The time step is $0.000932082\omega_p^{-1} \approx 52.25$ as, corresponding to a length of 15.66 nm. The number of particles per cell is 4 for the plasma and 256 for the witness electron beam. To eliminate an artificial growth in electron beam emittance caused by numerical Cherenkov radiation (NCR) generated in the standard Yee field solver, a special NCR-suppressing solver [9] has been used for electromagnetic field calculations.

The parameters of the externally injected witness beam used in the simulation are defined based on the results of simulations [10] for the future ARES-linac at the SINBAD facility at the DESY Hamburg campus [11]. A full set of initial beam parameters is given in Table 1. An initial symmetric Gaussian distribution in coordinate and momentum space is assumed for the injected beam.

In PBAs, transverse matching of injected electron beams into the plasma focusing fields is vital for beam emittance growth control. Tailoring the longitudinal density profile of the plasma entrance and exit with smooth vacuum-plasma and plasma-vacuum transitions can be used to minimize the induced emittance growth during beam acceleration and extraction, as shown in [12 - 14]. In the considered case the following longitudinal plasma density profile for up- and down-ramps was implemented:

$$f(z) = \frac{1}{(1 \pm (z - z_{0,d|u})/l_{d|u})^2}.$$

Here $z_{0,u}$ and $z_{0,d}$ are the longitudinal coordinates of the start of the up-ramp and the down-ramp respectively; l_u and l_d are the optimized characteristic scale lengths of the plasma ramps given by

$$l_{d|u} = \beta_{p0}\sqrt{\left(\frac{(N+1)\pi}{\ln(\beta_{goal}/\beta_i)}\right)^2 + \frac{1}{4}} = \frac{L_{d|u}}{\beta_{goal}/\beta_i - 1},$$

where β_{p0} is the beta function of the matched electron beam in PBAs, $\beta_{p0} = \sqrt{\gamma_b c m_e/(ge)}$, with γ_b being the beam Lorentz factor and g being the transverse focusing field in the plasma; β_i is the initial beta function of the beam; β_{goal} is the beta function of the beam matched to the plasma section in the case of the plasma up-ramp and to the external focusing elements in the case of the down-ramp; $N = 0, 1, 2, \ldots$; L_u and L_d are the lengths of the plasma up-ramp and the down-ramp respectively. Such tailoring of the longitudinal density profile was analytically and numerically investigated in [14] for PBAs operating in the nonlinear regime and can be experimentally realized in appropriate gas capillaries [15].

Simulation results and longitudinal plasma profile parameters are summarized in Table 2. The evolution of the normalized transverse emittance, transverse RMS size, mean energy, relative energy spread and absolute energy spread of the electron beam during injection, acceleration and extraction from the plasma is presented in Fig. 1.

Table 2: Longitudinal plasma profile parameters and properties of the accelerated electron beam after extraction from the plasma.

Q [pC]	5.6
Peak current [kA]	1.1
$\bar{E}$ [MeV]	2503
$\Delta E/\bar{E}$ [%]	0.54
Relative slice energy spread [%]	0.022
$\sigma_{z;rms}$ [μm]	0.59
$\sigma_{x;rms}$ [μm]	0.98
$\epsilon_{n;x}$ [μm]	0.53
Slice emittance, $\epsilon_{slice,\ n;x}$ [μm]	0.49
L_u [mm] / l_u [mm]	3.85 / 0.52
Acceleration region length [mm]	67.22
L_d [mm] / l_d [mm]	6.46 / 2.18
Laser focal plane position [mm]	4.07

The results show that the use of a short plasma up-ramp at the beginning of the plasma allows the initial transverse size of the injected beam to be decreased to a value close to the matched one, as shown in Fig. 1 (a). Due to the imperfect matching, the accelerated electron beam develops a decoherence of particle betatron oscillations and beam envelope oscillations [16, 17] from the end of the plasma up-ramp, consequently leading to a small growth in transverse emittance with a rate of approximately 9 nm/cm. Therefore, the use of short plasma ramps, 3.85 mm in length at the beginning of the plasma and 6.46 mm at the plasma exit, provides sufficient control over the emittance growth throughout the propagation distance.

ISBN: 978-3-95450-184-7 doi:10.18429/JACoW-IPAC2018-TUPML041

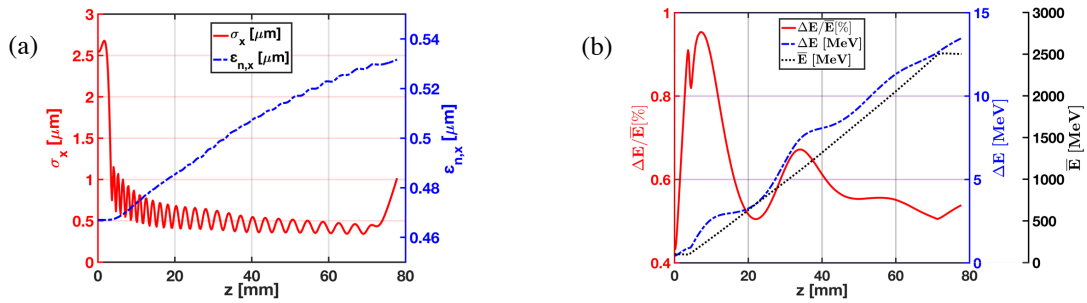

Figure 1: Evolution of the externally injected electron beam properties during acceleration to 2.5 GeV. Left panel (a): transverse RMS beam size (red solid curve); normalized transverse emittance (blue dashed curve). Right panel (b): relative energy spread (red solid curve); absolute energy spread (blue dashed curve); mean energy (black dotted curve).

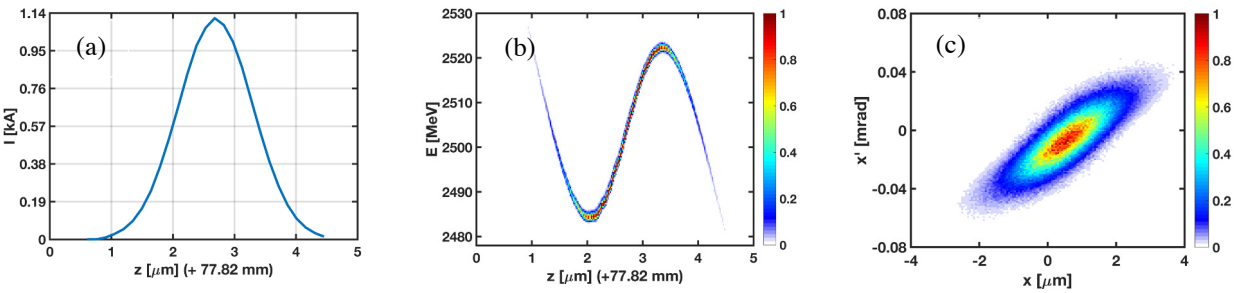

Figure 2: Current distribution (a), longitudinal (b) and transverse (c) phase-spaces of the accelerated electron beam after its extraction from the plasma target. The colormap describes normalized charge.

The energy spread of accelerated electron beams is determined to a considerable extent by the gradient of the longitudinal wakefield acting on them. In the present case, due to the short duration ($\sigma_{z;rms} \approx 2$ fs) and high density ($n_b = 5.7\times10^{17}$ cm^{-3}) of the electron beam, it creates its own wakefield, the beam loading field [18, 19], of the same order of magnitude as the gradient of the laser-excited plasma wakefield at the region occupied by the beam. Injection of the electron beam into a proper wave phase can allow the laser-driven wakefield to be compensated by the beam loading field, consequently leading to a mitigation of the energy spread growth during the acceleration process. As shown in Fig. 1 (b), throughout the up- and down-ramps the beam energy spread increases, as in regions of low density the beam loading field prevails over the laser-excited wakefield. The relative energy spread decreases in regions where the effective laser wakefield is flattened by the beam loading field, while the absolute energy spread stays near constant. However, in our case, periodical self-focusing and defocusing of the laser pulse are observed during its propagation through the parabolic plasma channel. This leads to periodic changes in the laser-excited wakefield amplitude and shape, and as a consequence, to a reduction of beam loading compensation due to the imperfect flattening of the field at the beam position.

Based on the above, the final properties of the accelerated electron beam are very promising (see Table 2) and meet the requirements of demanding applications such as FELs. The current distribution, as well as longitudinal and transverse phase-spaces of the accelerated electron beam after its extraction from the plasma are presented in Fig. 2.

We should note that a number of factors may have some effect on the results of the simulation. Numerical electron beam-laser dephasing of 12.17 µm (11 % of the plasma wavelength), observed in the simulations due to the superluminal group velocity of the laser pulse in the NCR-suppressing field solver [9], may affect the evolution of the electron beam properties to a small extent. Furthermore, a longitudinal energy chirp and beam asymmetry in the transverse plane, observed in the simulations for the ARES linac and not considered here, may have some influence on the evolution of the beam properties. 3D simulations with the full 6D phase space beam distribution are planned to examine these effects.

CONCLUSIONS

The successful quality-preserving acceleration of an externally injected beam by a laser wakefield accelerator was demonstrated through a two-dimensional PIC simulation. After extraction from the plasma the electron beam has very promising properties for FEL applications: mean energy of 2.5 GeV, beam RMS-duration around 2 fs, peak current of 1.1 kA, slice energy spread of 0.022 % and slice normalized transverse emittance of 0.49 µm.

It is planned to extend the presented studies on quality-preserving acceleration to electron beams with higher charges taking into account also the full 6D phase space beam distribution.

ISBN: 978-3-95450-184-7 doi:10.18429/JACoW-IPAC2018-TUPML041

ACKNOWLEDGEMENTS

We would like to acknowledge the OSIRIS Consortium (IST/UCLA) for providing access to the OSIRIS code. This work was supported by the European Unions Horizon 2020 research and innovation programme under grant agreement № 653782.

REFERENCES

[1] C. L. Haefner et al., "High average power, diode pumped petawatt laser systems: a new generation of lasers enabling precision science and commercial applications", in *Proc. SPIE Optics + Optoelectronics*, Prague, Czech Republic, April 2017, vol. 10241, p. 1024102, doi:10.1117/12.2281050

[2] K. Nakamura et al., "Diagnostics, Control and Performance Parameters for the BELLA High Repetition Rate Petawatt Class Laser", *EEE J. Quantum Electron*, vol. 53, no. 4, p. 1200121, 2017, doi:10.1109/JQE.2017.2708601

[3] E. Esarey, C. B. Schroeder and W. P. Leemans, "Physics of laser-driven plasma-based electron accelerators", *Rev. Mod. Phys*., vol. 81, pp. 1229 – 1285, 2009.

[4] W. P. Leemans et al., "Multi-GeV electron beams from capillary-discharge-guided subpetawatt laser pulses in the self-trapping regime", *Phys. Rev. Lett*., vol. 113, p. 245002, 2014.

[5] A. J. Gonsalves et al., "Generation and pointing stabilization of multi-GeV electron beams from a laser plasma accelerator driven in a pre-formed plasma waveguide", *Phys. Plasmas*, vol. 22, p. 056703, 2015.

[6] E. Svystun et al., "Beam quality preservation studies in a laser-plasma accelerator with external injection for EuPRAXIA", *Nucl. Instr. Meth. A*, in press, 2018, https://doi.org/10.1016/j.nima.2018.02.060

[7] P. A. Walker et al., "Horizon 2020 EuPRAXIA design study", *J. Phys.: Conf. Ser*., vol. 874, p. 012029, 2017.

[8] R. A. Fonseca et al., "OSIRIS: A three-dimensional, fully relativistic particle in cell code for modeling plasma based accelerators", *Lect. Notes Comput. Sci*., vol. 2331, pp. 342–351, 2002.

[9] R. Lehe, A. Lifschitz, C. Thaury, and V. Malka, "Numerical growth of emittance in simulations of laser-wakefield acceleration", *Phys. Rev. ST Accel. Beams*, vol. 16, p. 021301, 2013.

[10] J. Zhu, R. Assmann, U. Dorda and B. Marchetti, "Lattice design and start-to-end simulations for the ARES linac", *Nucl. Instr. Meth. A*, in press, 2018, https://doi.org/10.1016/j.nima.2018.02.045

[11]U. Dorda et al., "The Dedicated Accelerator R&D Facility Sinbad at DESY", in *Proc. IPAC'17*, Copenhagen, Denmark, May 2017, pp. 869-872, doi:10.18429/JACoW-IPAC2017-MOPVA012

[12] K. Floettmann, "Adiabatic matching section for plasma accelerated beams", *Phys. Rev. ST Accel. Beams*, vol. 17, p. 054402, 2014 https://doi.org/10.1103/PhysRevSTAB.17.054402

[13] I. Dornmair, K. Floettmann, and A. R. Maier, "Emittance conservation by tailored focusing profiles in a plasma accelerator", *Phys. Rev. ST Accel. Beams*, vol. 18, p. 041302, 2015.

[14] X. L. Xu et al., "Physics of phase space matching for staging plasma and traditional accelerator components using longitudinally tailored plasma profiles", *Phys. Rev. Lett*., vol. 116, p. 124801, 2016.

[15] L. Schaper et al., "Longitudinal gas-density profilometry for plasma-wakefield acceleration targets", *Nucl. Instr. Meth. A*, vol. 740, pp. 208-211, 2014, https://doi.org/10.1016/j.nima.2013.10.052

[16] K. A. Marsh et al., "Beam Matching to a Plasma Wake Field Accelerator using a Ramped Density Profile at the Plasma Boundary", in *Proc. PAC'05* (IEEE, Piscataway, NJ, 2005), Knoxville, TN, May 2005, pp. 2702–2704, doi:10.1109/PAC.2005.1591234

[17] A. G. Khachatryan, A. Irman, F. van Goor and K.-J. Boller, "Femtosecond electron-bunch dynamics in laser wakefields and vacuum", *Phys. Rev. ST Accel. Beams*, vol. 10, p. 121301, 2007. doi:10.1103/PhysRevSTAB.10.121301

[18] S. van der Meer, "Improving the power efficiency of the plasma wakefield accelerator", CERN-PS-85-65-AA, CLIC-Note-3, pp. 1-7, 1985.

[19] T. Katsouleas et al., "Beam loading in plasma accelerators", *Particle Accelerators*, vol. 22, pp. 81–99, 1987.